resources

MDPI

Article

The Assessment of the Usefulness of *Miscanthus* x *giganteus* to Water and Soil Protection against Erosive Degradation

Andrzej Mazur and Alina Kowalczyk-Juśko *

Department of Environmental Engineering and Geodesy, University of Life Sciences in Lublin, Leszczyńskiego 7, 20-069 Lublin, Poland; andrzej.mazur@up.lublin.pl
* Correspondence: alina.jusko@up.lublin.pl

Abstract: Water erosion is one of the major factors of soil degradation in the world. Various methods have been developed to prevent soil erosion. One of them is the use of anti-erosion belts on slopes, but it has both positive and negative effects. In order to minimize the negative effects, this study proposes the use of perennial grass in place of the most commonly used trees and shrubs. The paper presents studies on the erosion control effectiveness of a strip planted with *Miscanthus* x *giganteus*, established on a loess slope. Surface runoff of water and its constituents and erosion damage was studied on the experimental plot with a separate anti-erosion belt and the control plot. Obtained results indicate the anti-erosion efficiency of the established strip in the context of soil protection from water erosion and surface water protection from pollution, although, in the first years of vegetation, miscanthus has not yet reached the stage of full development. The average surface water runoff relating to precipitation causing the erosive event was 17.1% higher in the control plot than in the experimental plot. The volume of erosion damage in the form of rill erosion was 89.3% higher in the control plot. On the other hand, the volume of erosion damages in surface erosion and patches of deposited silts was lower by 14.7% and 21.6%, respectively. Soil losses from the control plot were 29% higher than those from the experimental plot. Dissolved plant nutrient runoff was also higher from the control plot by: 33.4% N-Ntot, 31.3% N-NH_4, 42.7% N-NO_3, 21.6% N-NO_2, 22.9% P-Ptot, 24.1% K.

Keywords: soil degradation; soil erosion; erosion damages; erosion control; arable land; anti-erosion strip; soil and water protection; *Miscanthus* x *giganteus*

Citation: Mazur, A.; Kowalczyk-Juśko, A. The Assessment of the Usefulness of *Miscanthus* x *giganteus* to Water and Soil Protection against Erosive Degradation. *Resources* **2021**, *10*, 66. https://doi.org/10.3390/resources10070066

Academic Editors: Demetrio Antonio Zema and Manuel Esteban Lucas-Borja

Received: 25 May 2021
Accepted: 20 June 2021
Published: 23 June 2021

1. Introduction

Water erosion is listed first among the factors degrading soils worldwide. Water erosion processes, besides transforming the relief [1], reduce humus compounds and plant nutrients from soils [2] and deteriorate the physical and chemical properties of soils [3]. It leads to reduced soil fertility [4] and decreased crop yields [5]. Water erosion also affects the deterioration of hydrological relations and increases flood risk and destruction of technical infrastructure facilities [6,7]. Nutrients eroded from agricultural land contribute to the eutrophication of surface waters [8–10]. Improperly used soil readily undergoes erosive degradation [11], and its restoration is complex, sometimes even impossible, because soil-forming processes are prolonged [12,13]. Soils formed from loess have been used agriculturally for years because they are among the most fertile soils globally [14], but they are characterized by potentially high susceptibility to water erosion [15].

Several methods have been developed to protect soil from water erosion. One of them is establishing mid-field erosion control strips constructed of appropriately selected tree and shrub species [16]. Studies have indicated a comprehensive, positive impact of strip plantings on mitigating climate change and preventing soil degradation [17]. There are also documented examples of their negative impact, e.g., decreased crop yields near established strips or weed infestation in adjacent farmland. A serious problem, especially in

herbal production, is the contamination of crops with fallen leaves [18]. Therefore, farmers are reluctant to introduce anti-erosion strips on their cultivated fields despite their many advantages, including protecting soils from water erosion.

In connection with the above, a concept was developed to create anti-erosion strips on production fields, located on slopes where the soils are highly endangered by water erosion. Instead of traditional anti-erosion strips, consisting of trees and shrubs, it has been proposed to use *Miscanthus* x *giganteus* Greef & Deuter—perennial clump grass with a height of up to 4 m. Miscanthus is mentioned among other perennial plant species as potentially useful in reducing the negative effects of soil erosion [19–23]. This species is characterized by low soil and agrotechnical requirements and gives high yields of up to 30 tons of dry matter (d.m.) ha^{-1} [24]. The advantage of using this species to establish anti-erosion strips could be the lack of generative reproduction under Polish conditions (its seeds do not mature), which limits uncontrolled spread. The risk of miscanthus spreading to neighboring fields is also minimized because, as a bunchgrass, this species does not develop long rhizomes, as is the case with *Miscanthus sacchariflorus* [25]. The aboveground parts of this grass dry out in late fall, and the leaves do not fall until winter, which would avoid problems with crop contamination in crops adjacent to erosion control strips. At the same time, *Miscanthus giganteus* already in the first year of vegetation can produce a significant mass of underground organs: roots and short, vigorous rhizomes, which can rapidly strengthen the topsoil. More intensive growth of miscanthus organs is observed in subsequent years. As a plant from the grass family, miscanthus annually recreates the aboveground mass, so it is advisable to harvest the aboveground parts in winter or early spring, before vegetation starts (February/March). Most often, the aboveground mass of plants is used in the energy industry in thermochemical (combustion, gasification, pyrolysis) and biochemical processes (methane fermentation) [26–28].

This paper presents empirical results from 2018–2019 on soil erosion rates and the suitability of giant miscanthus (*Miscanthus* x *giganteus* Greef & Deuter) to establish erosion control strips in the zone of eroded loess slopes to protect soils from water erosion and waters from pollution.

2. Materials and Methods

2.1. Location of the Research Facility

The study site is located in southeastern Poland in Czesławice (51°18′10″ N, 22°15′09″ E) (Figure 1a) in the Lublin Upland (Figure 1b), in the central part of the mesoregion—Naleczow Plateau (Figure 1c) [29].

In terms of relief, this area is typical for the loess soil of Lublin Upland. The Naleczow Plateau is the northwestern part of the Lublin Upland. The top layer of the Earth's surface is a thick loess cover, resting on the Upper Cretaceous strata, degraded moraine, sands, and gravels of glaciofluvial origin. Absolute heights here reach over 200 m (maximum 253 m). The Naleczow Plateau descends in two parallel steps from 20 to 30 m in the north towards the Lubartow Plateau and south towards the Belzec Plain. The Bystrzyca River valley is the eastern border, and the Vistula River valley is the western one. It covers an area of 625 km^2. Three longitudinal river valleys cut it: the Bystra, the Ciemięga, and the Czechówka. Due to its fertile loess soils, almost entirely under cultivation, they are forestless and densely populated [29]. The conditions described above mean that the Naleczow Plateau is strongly threatened by water erosion, confirmed by the dense network of existing gullies. Around the village of Parchatka near the Vistula valley, the density of the gully network is 11.25 km km^{-2} (this is the highest indicator in Europe). Wind erosion hardly contributes to soil degradation in the study area.

The experiment was established in Naleczow Plateau, on a convex–concave slope, in an eroded production field with a southeastern exposure. The experiment was located in the upper, convex part of the slope, where the slope exceeds 15%. The slope is about 60 m long and ends at the base with a drainage band ditch about 1.3 m deep and 3.5 m wide, which receives surface runoff water from the slope (Figure 2). Due to the presence of very

fertile loess soils, intensive plant production is carried out in the production field, where the experiment was established. The soils have been arable for many years, dominated by the cultivation of cereals, rape, maize, and root crops, which poorly protect the soil against water erosion. Winter wheat was grown in the production field in 2018 and winter rape in 2019.

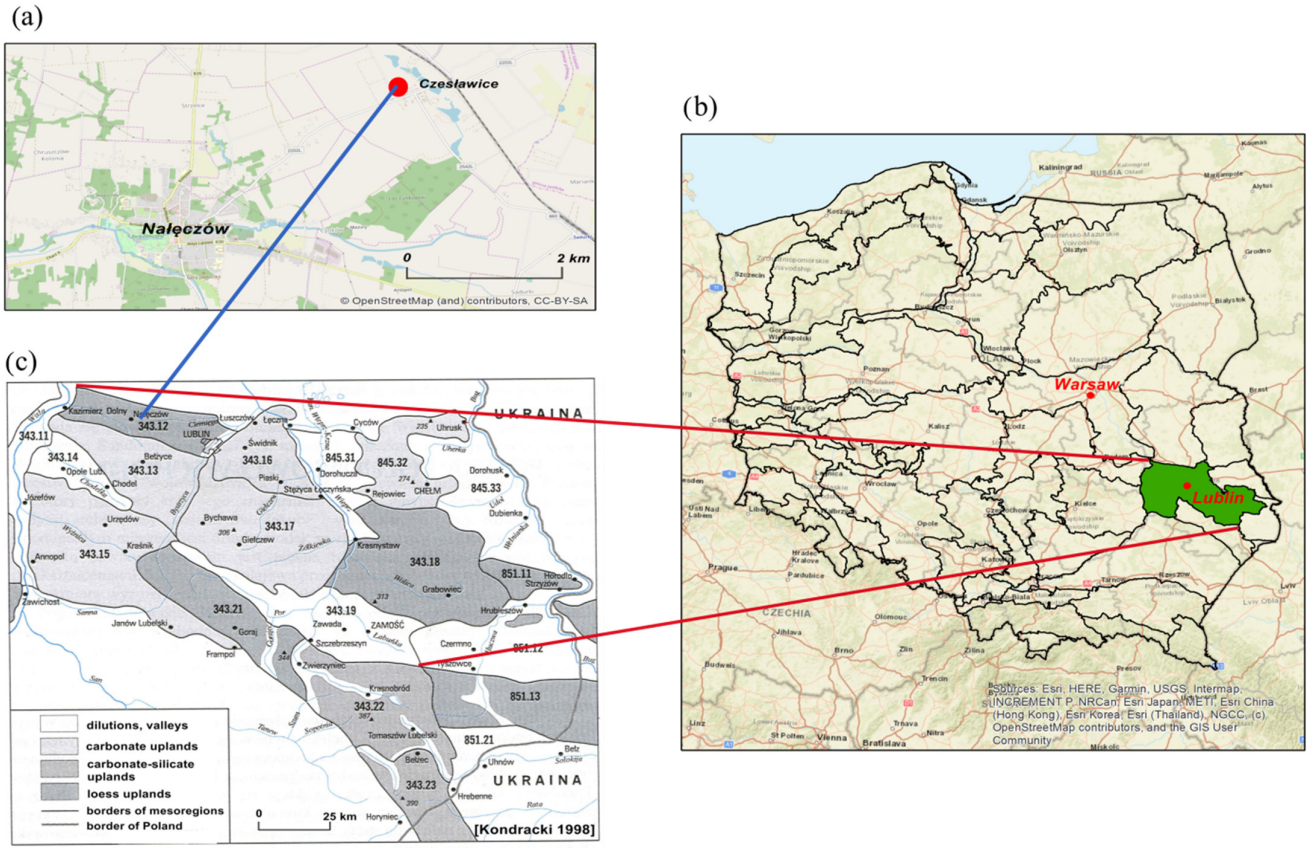

Figure 1. Location of the research facility (**a**) in Naleczow commune; (**b**) in Poland; (**c**) in Lublin Upland.

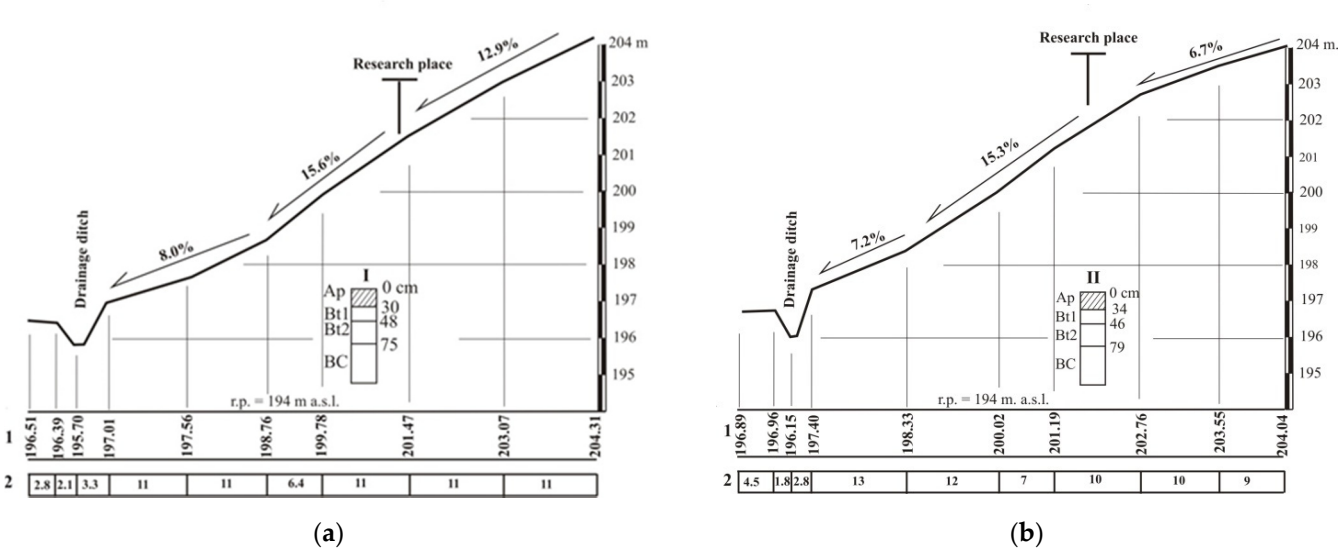

Figure 2. Cross-sections of the slope where the experimental plot with miscanthus planting (**a**) and the control plot (**b**) were established; 1—ground ordinates in meters, 2—distances in meters.

2.2. Description of the Experiment

Two adjacent plots of 300 m^2 each (15 m × 20 m) were separated on the slope. In the upper part of one of the separated plots, at the beginning of May 2018, transverse to the slope of the terrain, a 15 m × 2 m anti-erosion strip was separated, on which a perennial grass—*Miscanthus* x *giganteus*—was planted (experimental plot). The planting was made in a 25 cm × 25 cm grid. Vegetative seedlings were planted manually. Manual weeding was used. No mineral fertilizers were used. Pesticides were also not used because no pathogens were observed. The second plot was left unplanted (control plot). Both plots were maintained in black fallow. Plots were deliberately located on one production field, thanks to which they had similar topographical, soil, agrotechnical, and meteorological conditions. The maximum slope in the experimental plot location was 15.6%, and in the control plot slope, it was 15.3% (Figure 2). The average slopes were 11.7% and 10.8%, respectively. There were differences in the slopes above the experimental and control plots, which amounted to 12.9% and 6.7%, respectively, which could differentiate some physicochemical properties of the soil, e.g., pH or P content. Due to the fact that the experiment was conducted in natural conditions, it was difficult to select objects with identical parameters in terms of terrain, and the focus was mainly on the location of plots on a slope with a similar slope.

2.3. Soil Research

Soil samples for the study were collected in early May 2018 during the installation of the runoff capture devices. In both plots (experimental and control), one soil discovery was made each. The descriptions of the soil profiles were done in the field based on stratifying the distinguished diagnostic levels [30]. Soil samples were collected from each diagnostic level and determined according to recommended methods [31,32]:

- Granulometric composition—by Bouyoucos' areometric method as modified by Casagrande and Prószynski;
- The solid-phase density of soil—by pycnometry;
- Bulk density of soil—by weight (after collecting soil of intact structure into metal cylinders);
- Total porosity (P_o) was calculated from the formula:

$$P_o = \frac{\rho - \rho_o}{\rho} \quad (1)$$

where: ρ—solid-phase density,
ρ_o—bulk density of soil,

- Water permeability coefficient—using the Eijkelkamp apparatus (after taking soil of intact structure to metal cylinders);
- Content of: total Kjeldahl nitrogen, available phosphorus (P), potassium (K), calcium (Ca), total organic carbon (TOC);
- pH.

2.4. Research on the Biomass of Giant Miscanthus

At the end of each growing season, measurements of shoot height, thickness and abundance, and root length were made on 20 randomly selected miscanthus plants. Biomass samples were taken from 3 randomly selected sites on the anti-erosion strip, each with an area of 1 m^2, to determine fresh and dry matter yield and yield structure (leaves and stems). Biomass moisture content was determined according to EN ISO 18134-3:2015 [33].

2.5. Rainfall Research

Precipitation amounts were recorded during the growing season (from April to September) at a meteorological station equipped with a Hellmann's rain gauge, which was established near the experimental field. Studies of runoff and erosion damage in the plots were carried out during their occurrence (a total of 13 periods: 6 times in 2018 and

7 times in 2019). The dates of occurrence of erosion events against the rainfall height are shown in Table 1. The average air temperature and wind speed during the research period against the background of the averages over many years, obtained from the meteorological station in Radawiec, located approx. 16 km from the research site, are summarized in in Section 3.3.

Table 1. Date of occurrence events and amount of erosive precipitation.

Month	2018		2019	
	Day	Rainfall (mm)	Day	Rainfall (mm)
April	-	-	28	16.9
May	16	14.0	15	22.7
	17	26.0	20	24.6
June	28	21.3	21	17.5
July	16	18.4	-	-
August	-	-	12	26.2
			20	18.6
Sepetmber	4	13.5	2	26.8
	24	15.2		

2.6. Water Research

Methods described in Mazur [2] were used to capture and test water from surface and intrasoil runoff. A schematic drawing of the runoff interceptors is shown in Figure 3. In May 2018, a catcher for the surface and subsurface runoff in the slope to a depth of 0.75 m was installed. The author's catchers, structurally similar to a Gerlach catcher, was housed in the soil outcrop. Its volume was measured and taken in 1 L water bathymeters for laboratory analysis after the homogenization of the whole volume in the outflow presence. The content of suspensions in the collected water samples was determined according to Brański [34], employing the gravimetric method, and the nitrogen (total, ammonium, nitrate, and nitrite), phosphorus, and potassium were determined by applying the photometric method [35]:

- Total nitrogen (N-Ntot): WTW photometer model MPM 2010 (after oxidation of the test sample in thermo-reactor at the temperature 100 °C);
- Ammonium ($N\text{-}NH_4$) and nitrite ($N\text{-}NO_2$): WTW photometer model MPM 2010;
- Nitrate ($N\text{-}NO_3$), phosphorus (P-Ptot), and potassium (K): Slandi photometer model LF 300.

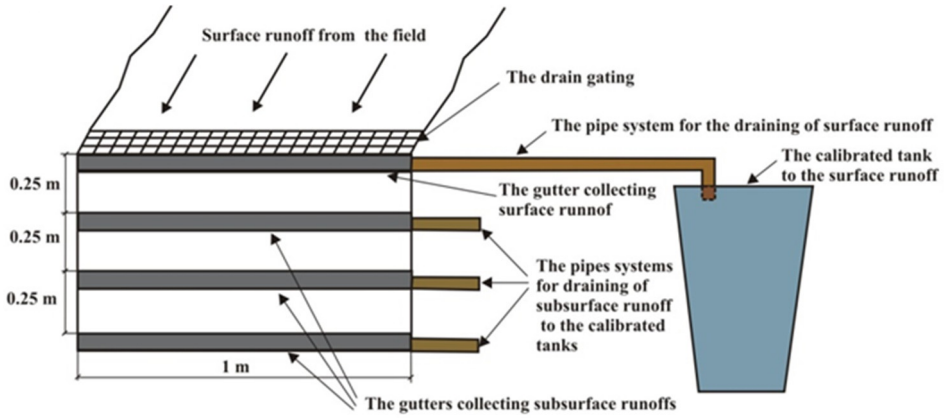

Figure 3. Schema of the catcher surface and subsurface runoff [2].

Based on constituent concentrations and runoff volumes, loads of constituents transported with water were determined.

2.7. Erosion Research

Qualitative–quantitative studies of the intensity of geomorphological processes were conducted after each surface runoff of water, according to the methodology developed by Mazur and Pałys [36]. The basis of the field study was the recognition of erosion forms in the form of linear erosion, rill erosion, and patches of deposited silts and their tabulations to calculate the volume of displaced soil. The basis of the field research was the recognition of erosive forms in the form of:

- Linear (groove) erosion, which consists of a shallow, linear washing of the upper levels of the soil profile by water flowing down the slope in the form of small water streams;
- Surface erosion—this is the washing and washing of the top layers of soil by water flowing on the surface of the slope;
- Patches of deposited sediment, which are formed as a result of the deposition of eroded soil material.

The quantitative list of inventoried erosion damage was tabulated and the volume of displaced soil was calculated.

3. Results and Discussion

3.1. Soil Properties

In the study site, there are soils formed from loess of the Haplic Luvisols type. These are poorly eroded soils of the Ap-B1t-B2t-BC-Cca profile structure, in which the arable and pristine horizon was formed from the B1t horizon. The location of the soil outcrops in the slope relief is shown in Figure 2. No skeletal fractions and very coarse sand were found in their composition. The remaining sand fractions (coarse, medium, fine, and very fine) account for 13% to 19% of the composition (Table 2). The dominant fraction in the granulometric composition is the dust fraction, which accounts for about 66% to 72% of the volume of soil samples, of which coarse dust constitutes from 41% to 48%.

Table 2. Granulometric composition of soils in the experimental and control plots.

Horizon	Depth (cm)	Percentage of Fractions with Diameter (mm)						
		1.0–0.5	0.5–0.25	0.25–0.1	0.1–0.05	0.05–0.02	0.02–0.002	≤0.002
Experimental plot								
Ap	0–30	0.2	0.8	1.3	14.7	47	25	11
B1t	30–48	0.2	0.2	0.7	12.9	44	27	15
B2t	48–75	0	0.2	0.6	14.2	42	25	18
BC	75–120	0	0.1	0.3	12.6	41	29	17
C_{Ca}	>120	0	0.1	0.2	12.7	40	30	17
Control plot								
Ap	0–34	0.3	0.7	1.5	16.5	48	23	10
B1t	34–46	0.2	0.3	0.8	14.7	46	22	16
B2t	46–79	0.1	0.2	0.5	15.2	44	22	18
BC	79–124	0	0.2	0.2	13.6	42	25	19
C_{Ca}	>124	0	0.1	0.2	13.7	41	27	18

On the other hand, the clay fraction represents 10% to 19% of the volume of the tested samples. The investigated soils of both plots have very similar granulometric composition, resulting from their vicinity. These soils can be classified as a granulometric group—dust, granulometric subgroup—clay dust (horizon Ap), and deeper layers—clay dust. The granulometric composition of the studied soils turned out to be typical for soils developed from loess in the Lublin Upland [2,37].

Water erosion hazard is highly dependent on soil physical properties [3,38,39]. The specific density of the studied soils was close to the value of 2.6 Mg m^{-3}. Its lower value was found in the plow-podzolic horizon (Ap) and it was higher in deeper levels (Table 3). A similar distribution was obtained for bulk density. The highest total porosity was found in the Ap horizon. It decreased with increasing depth. In terms of physical properties, the soils studied are typical of loess soils in the Lublin Upland [37,40]. The results in Table 3 indicate no adverse compaction of the solid phase below the reach of the working bodies of tillage implements, called plow sole. The formation of a plow sole in the production field was prevented by subsoiling to a depth of 50 cm every 4 years. The plow sole reduces water infiltration and accelerates water runoff [2,41,42], especially during heavy rainfall. In the arable layer, the water permeability coefficient was $6.452 \cdot 10^{-6}$ m s^{-1}. In deeper layers, it decreased and oscillated between 3.348 and $3.748 \cdot 10^{-6}$ m s^{-1}.

Table 3. Selected physical properties of the studied soils.

Horizon	Depth (cm)	Specific Density (Mg m^{-3})	Bulk Density (Mg m^{-3})	Total Porosity (%)	Water Permeability ($\times 10^{-6}$ m s^{-1})
Experimental plot					
Ap	0–30	2.54	1.42	44.1	6.452
B1t	30–48	2.62	1.55	42.1	3.351
B2t	48–75	2.63	1.51	42.6	3.410
BC	75–120	2.66	1.60	39.8	3.687
C_{Ca}	>120	2.65	1.65	37.7	3.745
Control plot					
Ap	0–34	2.58	1.42	45.0	6.551
B1t	34–46	2.64	1.52	40.6	3.512
B2t	46–79	2.66	1.59	40.2	3.348
BC	79–124	2.63	1.58	39.9	3.541
C_{Ca}	>124	2.64	1.64	37.9	3.748

The plow-podzolic horizon (Ap) of the investigated soils showed the highest abundance of nutrients (Table 4). Significant differences in phosphorus content were observed between plots and diagnostic levels. In the experimental plot, its maximum content in the Ap horizon was 11.3 mg P/100g soil (very high abundance), while in the control plot, it was 6.2 mg P/100g soil (medium abundance). Phosphorus content decreased with increasing depth and ranged from 1.9 to 5.7 mg P/100 g soil (deficient to medium abundance) in the deeper diagnostic levels. The potassium (1.5 to 3.0 mg K/100 g soil) and calcium (1.33 to 1.82 mg Ca/100 g soil) contents and pH values (5.2–5.7—slightly acidic reaction) varied to a lesser degree. Nitrogen content ranged from 0.009 to 0.101% and decreased with depth, as did TOC (0.35 to 1.21%).

3.2. Parameters of Miscanthus Biomass

Miscanthus seedlings in the first year after planting developed appropriately. Most plants produced single, delicate shoots that did not exceed 100 cm in height. In the second year of vegetation, the number of shoots produced from one seedling increased to 7.3 on average, and their heights exceeded 2 m (Table 5). It is a typical course of miscanthus development, which in subsequent years grows, produces a higher number of shoots, and forms a dense canopy [24]. The underground parts of the plants, consisting of roots and rhizomes, were primarily located in the arable layer, reaching an average depth of 16.9 and 20.1 cm in the first and second year of vegetation, respectively. The root system of miscanthus, also in subsequent years of development, is not very deep [43].

In contrast, in the arable layer of soil, numerous roots and rhizomes provided with growth buds were tangled, which on the one hand makes it difficult to obtain material for propagation, and on the other hand, binds the soil and does not allow it to be carried

away by water or wind erosion. Monti and Zatta [43] observed that soil penetration by miscanthus roots was extremely shallow—almost 90% of the total roots were in a layer ≤0.35 m. In a study by Mann et al. [44], miscanthus roots, after reaching a depth of slightly less than 50 cm, did not penetrate deeper soil layers. In contrast, Neukirchen et al. [45] found that 28% of miscanthus root biomass was located in the upper 0.30 m of soil.

Table 4. Macronutrient contents, total organic carbon (TOC), and pH_{-KCl} values in soils.

Horizon	Kjeldahl Nitrogen (%)	P	K	Ca	pH_{-KCl}	TOC (%)
		(mg/100 g Soil)				
Experimental plot						
Ap	0.101	11.3	2.98	1.65	6.3	1.16
B1t	0.074	9.9	1.72	1.33	5.2	0.44
B2t	0.017	4.8	2.52	1.82	6.1	0.48
BC	0.011	2.0	2.30	1.58	6.3	0.48
C_{Ca}	0.009	2.1	2.21	1.59	6.3	0.35
Control plot						
Ap	0.080	6.2	2.51	1.57	5.6	1.21
B1t	0.079	5.7	2.45	1.56	5.2	1.21
B2t	0.012	1.9	1.51	1.40	5.7	0.76
BC	0.012	2.0	2.05	1.74	5.7	0.62
C_{Ca}	0.010	2.0	1.95	1.68	5.8	0.54

Table 5. Biometric parameters of giant miscanthus in the first (I) and second (II) year of vegetation.

Parameter		Mean	Standard Deviation	Variability	Minimum	Maximum
Shoot height (cm)	I	98.4	17.0	0.17	75.0	128.0
	II	202.0	11.7	0.06	184.0	226.0
Shoot number (pcs.)	I	1.5	0.7	0.46	1.0	3.0
	II	7.3	2.8	0.39	1.0	12.0
Shoot thickness (mm)	I	4.3	1.2	0.28	2.0	6.5
	II	5.1	0.9	0.18	3.0	6.6
Root length (cm)	I	16.9	3.4	0.20	12.0	23.0
	II	20.1	4.1	0.20	13.0	27.0

I—the first year of vegetation, II—the second year of vegetation.

The soil-protective function of *Miscanthus giganteus* is also to protect the soil surface against splash erosion—the initial stage of water erosion. It is the effect of various plants taking over the kinetic energy of falling raindrops [46,47]. This effect persisted in the autumn–winter period because the leaves of *Miscanthus*, despite drying out, remained on the plants, protecting the soil against rainfall. The leaves remaining on the stems for a long time did not pollute the adjacent fields. Undesirable spread of miscanthus plants to adjacent fields was not observed.

Yearly miscanthus plants produced a small aboveground mass averaging 340.21 g m^{-2} fresh matter (234.88 g m^{-2} dry matter). The dominant component of the yield was leaves, whose percentage share in fresh and dry matter was 64.45% and 72.41%, respectively. Miscanthus in the second growing year had a higher yield: an average of 1183.53 g m^{-2} fresh weight (939.14 g m^{-2} dry matter) and a stronger dominance of shoots, which accounted for 71.33% and 67.39% of the fresh and dry matter yield, respectively (Figure 4). Despite the end of the growing cycle, giant miscanthus was characterized by relatively high moisture content, especially of the stems, at harvest time. The average dry matter content in the first year was 69.38% in whole plants, 76.36% in leaves, and only 56.58% in stems, while in

the second year, it was higher at 79.30%, 92.00%, and 76.33%. Similar data were presented by Clifton-Brown et al. [24], who found that *Miscanthus giganteus* in the second year of vegetation developed a higher number of shoots, which gave a higher yield compared to the first year, and their moisture content was lower.

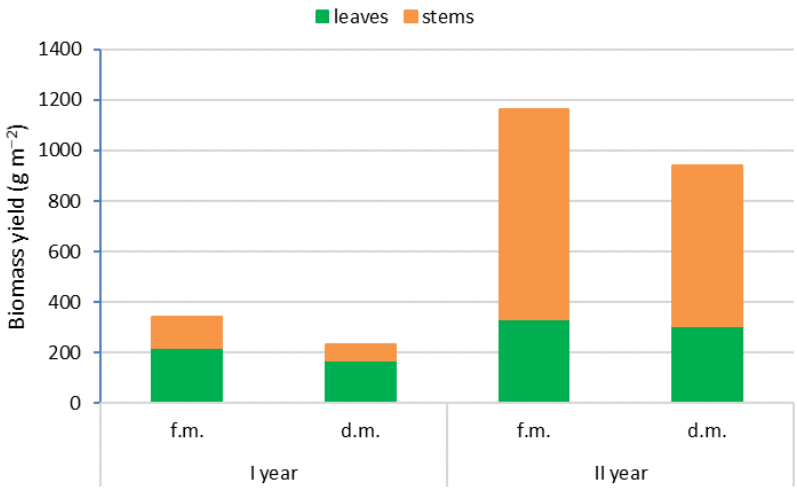

Figure 4. Fresh matter (f.m.) and dry matter (d.m.) yield of giant miscanthus.

3.3. Meteorological Conditions

The intensity of water erosion depends on climatic conditions, especially the amount and intensity of precipitation [48], as well as air temperature and wind speed. Precipitation recharge during the growing season of plants at the study site is presented in Table 6. During the study period, the highest monthly precipitation was recorded in May 2019 (95.2 mm) and was about 64.7% higher than the multi-year average monthly precipitation. In contrast, the lowest rainfall was recorded in June 2019 (18.8 mm) and accounted for 26.9% of the average monthly rainfall. During the growing season, both 2018 and 2019 precipitation was lower than the multi-year average precipitation by 13.4% and 18.8%, respectively. The highest average monthly air temperature during the study period was recorded in August 2018 (20.2 °C) and was approximately 9.8% higher than the multi-year average. On the other hand, the lowest temperature was recorded in April 2019 (9.4 °C) and was 9.3% higher than the multi-year average. In terms of average air temperature, the growing season in 2018 was warmer by approx. 20% compared to the multi-year average, and in 2019 by approx. 8.6% (Table 6). The average wind speed in the region where the research was conducted was not very differentiated in individual months and during the research period (as well as in many other years) it ranged from 2.1–3.4 m s^{-1} (Table 6).

The course of meteorological conditions significantly affects the intensity of soil erosion, especially the amount of precipitation, its intensity, and kinetic energy [2,48,49]. In the study, no high precipitation was recorded during which strong water erosion processes would be activated. Studies on the outflow of water and matter components and records of erosion damage in plots were carried out in the rainfall range from 13.5 to 26.8 mm (Table 1). The calculated coefficient of precipitation variation was 23.9% (Table 7)—average variability [50]. According to the study conducted by Mazur [2], single erosive precipitation can reach up to 63.6 mm. It is already catastrophic precipitation, during which sizeable erosive damage occurs. Erosive rainfall occurred most frequently in May (30.1%) and September (23.1%). Their frequencies were 15.4% in June and August, and in April and July, 7.7% (Table 1).

3.4. Water Outflow and Selected Matter Components

Surface runoff and analyzed water quality indicators of surface runoff from the plots are presented in Table 7. Intrasoil runoff was not observed.

Table 6. Meteorological conditions during study years and multi-year averages.

Year	Month							
	IV	**V**	**VI**	**VII**	**VIII**	**IX**	**X**	
	Precipitation (mm)							∑ **IV-X**
2018	54.6	49.4	48.1	84.6	23.6	51.6	42.9	354.8
2019	32.1	95.2	18.8	26.5	81.6	48.6	30.1	332.9
Average 1961–2010 *	41.6	57.8	69.9	77.3	66.6	56.5	40.2	409.9
	Temperature (°C)							$\overline{x}$
2018	13.0	16.7	18.3	19.9	20.2	15.3	9.8	16.8
2019	9.4	12.8	21.3	18.3	19.7	14.1	10.5	15.2
Average 1961–2010 *	8.6	13.6	16.9	18.9	18.4	13.4	8.2	14.0
	Wind (m s^{-1})							$\overline{x}$
2018	3.3	2.4	2.2	2.7	2.2	2.2	2.7	2.5
2019	3.4	2.9	2.6	2.8	2.0	2.7	2.1	2.6
Average 1961–2010 *	3.2	2.7	2.6	2.5	2.4	2.5	2.9	2.7

* Source—Institute of Meteorology and Water Management—National Research Institute, Warsaw.

Table 7. Indicators characterizing rainfall, surface runoff, and erosion damage.

Indicator		Medium	Standard Deviation	Variation	Minimum	Maximum
Rainfall (mm)		20.1	4.8	23.9	13.5	26.8
Outflow (mm)	a	3.5	1.4	40.0	1.0	5.4
	b	4.1	1.8	43.9	1.3	6.6
Soil suspension (g dm^{-3})	a	36.184	27.115	74.9	2.321	75.312
	b	40.547	29.384	72.5	1.331	88.325
N-Ntot (mg dm^{-3})	a	10.439	3.528	34.0	5.023	15.854
	b	11.871	3.356	28.3	6.123	16.621
$N\text{-}NH_4$ (mg dm^{-3})	a	5.152	1.662	32.3	2.498	7.534
	b	5.770	1.646	28.5	3.512	7.985
$N\text{-}NO_3$ (mg dm^{-3})	a	2.644	1.176	44.5	1.215	4.613
	b	3.109	1.179	37.9	1.115	4.954
$N\text{-}NO_2$ (mg dm^{-3})	a	1.649	0.521	31.6	0.956	2.325
	b	1.747	0.471	27.0	0.756	2.325
P-Ptot (mg dm^{-3})	a	0.818	0.232	28.4	0.539	1.241
	b	0.872	0.227	26.0	0.583	1.273
K (mg dm^{-3})	a	9.051	2.441	27.0	4.124	14.128
	b	9.783	2.559	26.2	4.984	15.228
Volume of rills (m^3 ha^{-1})	a	0.18	0.12	66.7	0.05	0.36
	b	0.34	0.27	79.4	0.03	0.78
Surface wash (m^3 ha^{-1})	a	0.28	0.21	75.0	0.06	0.72
	b	0.24	0.16	66.7	0.09	0.48
Mud volume (m^3 ha^{-1})	a	0.12	0.10	83.3	0.03	0.31
	b	0.10	0.05	50.0	0.03	0.17

a—experimental plot, b—control plot.

The variability of surface water runoff was 40% in the experimental plot (average variability) and 43.9% in the control plot (high variability) [50]. Surface water runoff from the experimental plot ranged from 1.0 to 5.4 mm (Table 7), accounting for 7.4% to 20.6% of the precipitation causing the erosion event. In the control plot, the runoff was higher, ranging from 1.1 to 6.6 mm, accounting for 9.3% to 25.2% of the precipitation. These

rates were low compared to the maximum surface runoff on arable land, accounting for more than 40% of the precipitation causing an erosion event [32]. The experimental plot received a total of 45.6 mm of water column runoff during the study period, and the control plot received 52.7 mm. The study results show that not consistently high rainfall gives high surface runoff (Figure 5a,b). However, the obtained correlation coefficients r = 0.82 and r = 0.76 in the experimental and control plots, respectively (determination coefficients R^2 = 0.67 and R^2 = 0.60, respectively), show that the amount of surface runoff is very strongly correlated with the amount of precipitation. Studies conducted by Kim et al. [51] and Zhang et al. [52] demonstrated that several other factors, such as precipitation intensity, vegetation cover, and soil moisture, affect the amount of runoff. However, it is mainly the amount and intensity of precipitation that initiates surface runoff.

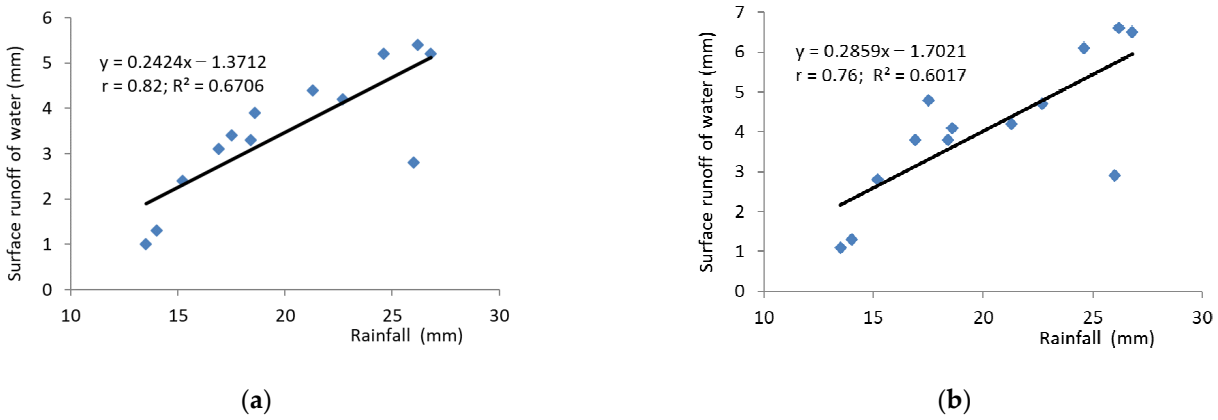

Figure 5. Surface runoff of water depending on the rainfall amount; (**a**) experimental plot, (**b**) control plot.

Surface runoff water from the slope carries dissolved or suspended matter components [53]. Under the conditions of the present study, the concentration of soil-suspended solids contained in the runoff water from the experimental plot ranged from 2.321 to 75.312 g dm^{-3} (Table 7) and was characterized by high variability (74.9%) [50]. In the control plot, soil-suspended solid concentrations ranged from 1.331 to 88.325 g dm^{-3}, and the variability was 72.5% (high variability) [50]. The maximum values of soil suspended solid concentrations in waters flowing away from the slope are not the highest. Żmuda's study [49] showed that the concentration of soil-suspended solids can be as high as 236.228 g dm^{-3}. Figure 6 shows the relationships between soil surface scour and the amount of precipitation that causes erosion events. It shows that the response of soil to precipitation varies greatly, and the amount of soil scour cannot be inferred from precipitation volume. However, the mass of eroded soil appeared to be highly correlated with the amount of precipitation. In the experimental and control plots, the correlation coefficient was r = 0.89 and r = 0.87, respectively (coefficient of determination R^2 = 0.80 and R^2 = 0.76, respectively). The relationship between rainfall and mass eroded soil was the subject of research of many authors. Experiments in simulated conditions [54] showed that an increasing rainfall intensity had a larger effect on the sediment yield than an increasing slope. Other laboratory research [55] has suggested that the collected sediment yield and eroded soil volume increased with rainfall duration and slope.

Soil runoff on the slope during single erosion events varied widely and ranged from 0.030 to 2.386 Mg ha^{-1} in the experimental plot and from 0.383 to 4.066 Mg ha^{-1} in the control plot. Studies conducted by Żmuda [49] have shown that in root crops on the Trzebnickie Hills, the maximum surface soil washout during a single event can be as high as 60.132 Mg ha^{-1}. However, in the study carried out by Rejman [37] in the Lublin Upland, this value reached 20.640 Mg ha^{-1}. During the study period, soil surface washout on the experimental plot was 20.510 Mg ha^{-1}, while on the control plot, it was statistically significantly higher (about 29%) and amounted to 26.475 Mg ha^{-1} (Figure 7). The results

of the research prove that the anti-erosion strip used reduced the leaching of soil from the slope and limited the development of modern morphodynamic processes. The results obtained from field tests regarding soil loss are difficult to relate to other results. This is due to differences in the inclination of slopes and soil conditions, but mainly due to the erosive nature of rainfall. Research conducted by Gil [56,57] showed that even the average ten-year size of soil loss can differ by up to 140% for cereal crops and 50% for potato cultivation.

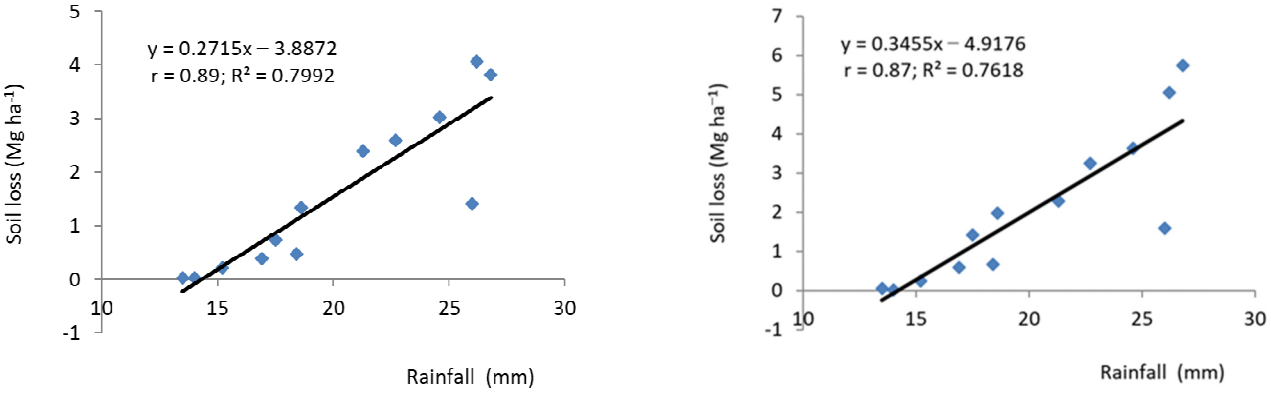

(**a**) (**b**)

Figure 6. Soil loss in dependence on the rainfall amount; (**a**) experimental plot, (**b**) control plot.

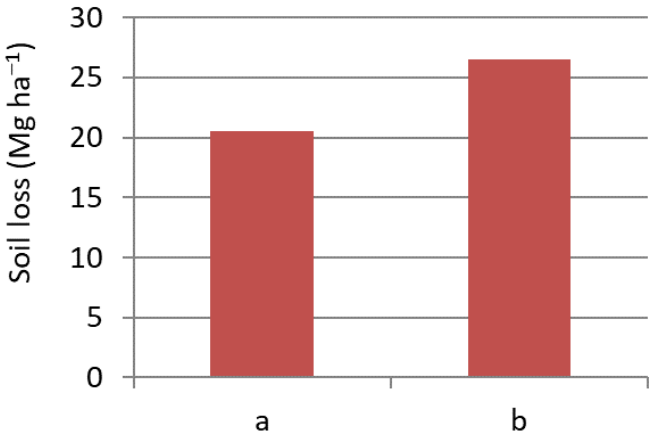

Figure 7. Soil losses during surface runoff; (**a**) experimental plot, (**b**) control plot.

The chemistry of waters draining from the slope varied widely, both among years and during periods of runoff occurrence (Table 7). Concentrations of total nitrogen in surface runoff water from the experimental plot ranged from 5.023 to 15.854 mg dm^{-3} N-Ntot. Concentrations of other forms of nitrogen were as follows: ammonium 2.498–7.534 mg dm^{-3} $N\text{-}NH_4$, nitrate 1.215–4.613 mg dm^{-3} $N\text{-}NO_3$, nitrite 0.956–2.325 mg dm^{-3} $N\text{-}NO_2$. The concentration of phosphorus runoff in dissolved form was 0.539–1.241 mg dm^{-3} P-Ptot, and potassium was 4.124–14.128 mg dm^{-3} K. Analyzing the obtained results of the chemistry of waters flowing away from the control plot (Table 7), it can be stated that the concentration of most of the examined chemical indicators of water quality was higher than in waters flowing away from the experimental plot. It applies to the maximum as well as average values. Concentrations of total nitrogen ranged from 6.123 to 16.621 mg dm^{-3} N-Ntot. The concentration of other forms of nitrogen was on the level of ammonium 3.512–7.985 mg dm^{-3} $N\text{-}NH_4$, nitrate 1.115–4.954 mg dm^{-3} $N\text{-}NO_3$, and nitrite 0.756–2.325 mg dm^{-3} $N\text{-}NO_2$. Dissolved effluent phosphorus concentration was 0.583–1.273 mg dm^{-3} P-Ptot, and potassium was 4.984–15.228 mg dm^{-3} K. Similar values

were obtained by Mazur [2] and Żmuda [49]. The studied chemical indicators of water quality, determined in waters flowing away from the experimental and control plots, were characterized by variability from 26.0% to 37.9% (Table 7)—average variability [50]. However, the average contents of biogenic components (phosphorus, total nitrogen, ammonium, and nitrite nitrogen) exceeded the limit values corresponding to a good class of surface water (Table 8) [58].

Table 8. The threshold values of water quality indices.

Index	Threshold Values	
	I Quality Class	**II Quality Class**
N-Ntot (mg dm^{-3})	≤1.8	≤3.0
$N\text{-}NH_4$ (mg dm^{-3})	≤0.13	≤0.30
$N\text{-}NO_3$ (mg dm^{-3})	≤1.3	≤2.0
P-Ptot (mg dm^{-3})	≤0.13	≤0.25

During single erosion events, the following flowed out of the experimental plot with water in the dissolved form: from 0.087 to 0.651 kg ha^{-1} N-Ntot, 0.039–0.318 kg ha^{-1} $N\text{-}NH_4$, 0.019–0.133 kg ha^{-1} $N\text{-}NO_3$, 0.016–0.104 kg ha^{-1} $N\text{-}NO_2$, 0.005–0.044 kg ha^{-1} P-Ptot, and 0.143–0.514 kg ha^{-1} K. From the control plot, plant nutrient runoff was higher during the study period and ranged from 0.104 to 0.853 kg ha^{-1} N-Ntot, 0.046–0.428 kg ha^{-1} $N\text{-}NH_4$, 0.022–0.241 kg ha^{-1} $N\text{-}NO_3$, 0.021–0.116 kg ha^{-1} $N\text{-}NO_2$, 0.007–0.056 kg ha^{-1} P-Ptot, and 0.087–0.623 kg ha^{-1} K. The concentrations of the studied chemical indicators of water quality were similar to the results obtained by Mazur [2] and Żmuda [49]. The experimental plot drained during the study period: 4.655 kg ha^{-1} N-Ntot, 2.314 kg ha^{-1} $N\text{-}NH_4$, 1.158 kg ha^{-1} $N\text{-}NO_3$, 0.745 kg ha^{-1} $N\text{-}NO_2$, 0.362 kg ha^{-1} P-Ptot, and 4.046 kg ha^{-1} K (Figure 8). Plant nutrient losses were higher from the control plot: 6.209 kg ha^{-1} N-Ntot, 3.038 kg ha^{-1} $N\text{-}NH_4$, 1.652 kg ha^{-1} $N\text{-}NO_3$, 0.906 kg ha^{-1} $N\text{-}NO_2$, 0.445 kg ha^{-1} P-Ptot, and 5.021 kg ha^{-1} K (Figure 8). The test results show that the anti-erosion strip that was used limited the loss of nutrients from the slope and turned out to be an effective solution in preventing, among others, contamination of surface waters with area pollution from agricultural land. The complexity of the problem makes it difficult to directly compare the results obtained with the results of erosion studies on other sites. The intensity of water erosion is determined by many local factors, e.g., erosivity of precipitation, erosive susceptibility of soils, relief, vegetation cover, land use, etc. [51,59,60]. These factors are interrelated and can enhance or reduce soil erosion. Kim et al. [51] determined nutrient losses of N-Ntot 5.63–13.97 kg ha^{-1} and P 0.96–11.00 kg ha^{-1}, depending on the location and method of use. On the other hand, studies conducted by Mazur [2], Żmuda [49], Koc [61], and Rajda et al. [62] showed that annual nutrient losses due to erosive processes can be: 4.5–20 kg ha^{-1} N-Ntot, 0.5 kg ha^{-1} P, and 2–17 kg ha^{-1} K.

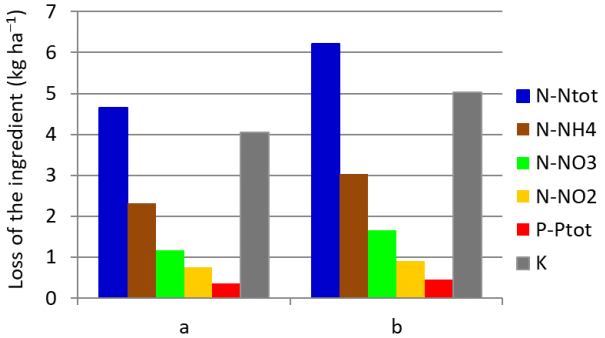

Figure 8. Mass of eroded chemical components; (**a**) experimental plot, (**b**) control plot.

The Pearson correlation coefficients between nutrient losses (N-Ntot, N-NH_4, N-NO_3, N-NO_2, P-Ptot, and K) and rainfall and surface water runoff were calculated (Table 9). The analysis of the relationship, at the significance level of $\alpha = 0.05$, showed statistically significant correlations between the analyzed factors at the high and very high levels [63].

Table 9. Correlation between loss of nutrients and rainfall and surface water runoff.

Indicator	Nutrient					
	N-Ntot (kg ha^{-1})	N-NH_4 (kg ha^{-1})	N-NO_3 (kg ha^{-1})	N-NO_2 (kg ha^{-1})	P-Ptot (kg ha^{-1})	K (kg ha^{-1})
	Experimental plot					
Rainfall (mm)	0.73	0.75	0.70	0.65	0.65	0.54
Outflow (mm)	0.75	0.77	0.63	0.76	0.78	0.73
	Control plot					
Rainfall (mm)	0.73	0.73	0.68	0.76	0.60	0.52
Outflow (mm)	0.85	0.84	0.81	0.85	0.79	0.75

3.5. Erosion Damage

Under the conditions of the present study, the recorded erosion damages in the experimental plot in the form of rill erosion, surface erosion, and patches of deposited silt varied between 0.05–0.36 m^3 ha^{-1}, 0.06–0.72 m^3 ha^{-1}, and 0.03–0.31 m^3 ha^{-1}, and had a variability from 66.7% to 83.3% (Table 7)—high variability [50]. In the control plot, the erosion damage was, respectively: 0.03–0.78 m^3 ha^{-1}, 0.09–0.48 m^3 ha^{-1}, and 0.03–0.17 m^3 ha^{-1}. Their variabilities ranged from 50.0% to 79.4%—also high variability [50]. During the two-year study period, the volume of inventoried erosion damage in the form of rill erosion in the experimental plot was 2.33 m^3 ha^{-1} (Figure 9). Surface erosion was estimated at 3.67 m^3 ha^{-1}, and the volume of patches of deposited silt was 1.62 m^3 ha^{-1}. In the control plot, the recorded volume of rill erosion was statistically significantly higher (about 89.3%) than in the experimental plot and amounted to 4.41 m^3 ha^{-1}. On the other hand, the surface erosion was smaller by 14.7% and amounted to 3.13 m^3 ha^{-1}. The volume of deposited silts was also smaller by 21.6% and amounted to 1.27 m^3 ha^{-1}. The slope above the control plot was almost two times smaller than that above the experimental plot (Figure 2). It is related to lower velocity and volume of surface water runoff and its lower eroding force [64,65]. Nevertheless, the volume of the eroded material in the form of groove and surface erosion was 26% higher in the control plot than in the experimental plot (Figure 9). Also, the mass of the eroded soil was 29% higher in the control plot than in the experimental plot (Figure 7). The results obtained show that the erosion control belt dispersed streams of water flowing down the slope, reducing the erosive energy. It is also visible in inventoried erosion damage, where in the control plot the dominant form was groove erosion, and in the experimental plot, surface erosion was, to a lesser extent, degrading the soil. The greater eroding power of flowing water in the control plot than in the experimental plot is also evidenced by the smaller volume of deposited sediments, as the flowing water in dense streams lifted the eroded soil material beyond the control plot. With concentrated water runoff, the eroded soil material is carried outside the slope zone and settles at their bases and in the bottoms of denudation valleys, which has also been described by other researchers [37,49,65,66]. The obtained indices characterizing the size of inventoried erosion damages were lower in relation to the data included in the bibliography, which was influenced by the lack of high-intensity precipitation. The study by Mazur [67] showed that in agricultural catchments, the annual volumes of erosion damage can amount to: 3.1 m^3 ha^{-1}—rill erosion, 2.2 m^3 ha^{-1}—surface erosion, 2.3 m^3 ha^{-1}—deposited silts. Considering that the study by Mazur [67] was carried out in the whole catchment area (including forested, sodded, and built-up areas, where the intensity of erosion is low), the obtained erosion rates per arable land only would be higher.

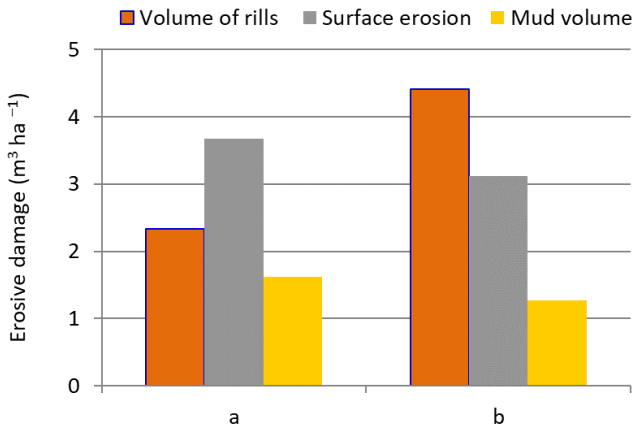

Figure 9. Inventory erosion damage; (**a**) experimental plot, (**b**) control plot.

The relationship between the amount of erosion damage and precipitation, and surface water runoff was best described by linear equations (Table 10). The obtained correlation coefficients $0.70 \leq r \leq 0.90$ (coefficients of determination $0.52 \leq R^2 \leq 0.81$) show that, according to the classification of Stanisz [63], the magnitude of erosion damage was high and very highly correlated with the amount of precipitation and the amount of water runoff in the experimental plot. Also, a high and very high correlation between the analyzed variables was obtained in the control plot, but the calculated correlation and determination coefficients were lower ($0.53 \leq r \leq 0.87$; $0.28 \leq R^2 \leq 0.75$). The high correlation between water erosion rate and rainfall and runoff parameters has also been indicated by studies of other authors [2,48,49].

Table 10. Equations of the dependence of the size of erosion damage on the amount of precipitation and surface water runoff.

Parameter	Rainfall (mm)	R^2	r	Runoff of Water (mm)	R^2	r
Experimental plot						
Volume of rills (m^3 ha^{-1})	y = 0.0182x − 0.1872	0.53	0.73	y = 0.0767x − 0.0896	0.81	0.90
Surface wash (m^3 ha^{-1})	y = 0.0366x − 0.4541	0.69	0.83	y = 0.125x − 0.1556	0.71	0.84
Mud volume (m^3 ha^{-1})	y = 0.0147x − 0.1713	0.52	0.72	y = 0.0568x − 0.0745	0.68	0.82
Control plot						
Volume of rills (m^3 ha^{-1})	y = 0.0364x − 0.394	0.42	0.65	y = 0.1316x − 0.1942	0.75	0.87
Surface wash (m^3 ha^{-1})	y = 0.0248x − 0.2583	0.56	0.75	y = 0.0592x + 0.0003	0.44	0.66
Mud volume (m^3 ha^{-1})	y = 0.0057x − 0.0181	0.28	0.53	y = 0.0223x + 0.007	0.58	0.76

4. Conclusions

Studies conducted on loess slope on the usefulness of *Miscanthus* x *giganteus* for the establishment of erosion control strips to protect soils from water erosion and waters from pollution proved that even in the first two years of vegetation, when miscanthus has not yet reached the stage of full development, a beneficial effect of the planted plants could be observed. The average surface water runoff relating to the precipitation causing the erosion event in the experimental and control plots was 17.4% and 20.4%, respectively. The volumes of inventoried erosion damage, in the form of rill erosion, were 89.3% higher in the control plot than in the experimental plot. However, the volumes of erosion damage in the form of

surface erosion and patches of deposited silt were lower by 14.7% and 21.6%, respectively. Soil losses during the study period were 29% higher from the control plot than from the experimental plot and amounted to 26.475 Mg ha^{-1} and 20.510 Mg ha^{-1}, respectively. Furthermore, concentrations of most of the studied chemical indicators of water quality in runoff from the control plot were higher than in runoff from the experimental plot. The outflow in the dissolved form of plant nutrients was higher from the control plot by 33.4% N-Ntot, 31.3% N-NH_4, 42.7% N-NO_3, 21.6% N-NO_2, 22.9% P-Ptot, 24.1% K than from the experimental plot.

The results obtained in the first two years of the experiment are promising and allow us to assume that the establishment of erosion control strips of miscanthus will enable adequate protection of soils from water erosion and waters from surface pollution originating from areas used for agricultural purposes. The continuation of the research will allow us to assess the usefulness of this new method of soil and water protection in the following years when miscanthus can reach its full development (both above and below ground). Continuation of the research in subsequent years will allow to verify the effectiveness of the method in the years with average and high rainfall, if any.

Author Contributions: Conceptualization: A.K.-J.; methodology, data collection, and original data analysis: A.M.; investigation, data presentation, writing, resources, and visualization: A.M. and A.K-J. All authors have read and agreed to the published version of the manuscript.

Funding: This research was funded from the 'Excellent science' program of the Ministry of Education and Science as a part of the contract no. DNK/SP/465641/2020 "The role of the agricultural engineering and environmental engineering in the sustainable agriculture development".

Institutional Review Board Statement: Not applicable.

Informed Consent Statement: Not applicable.

Conflicts of Interest: The authors declare no conflict of interest.

References

1. Young, F.J.; Hammer, R.D. Soil-landform relationship on a loess-mantled upland landscape in Missouri. *Soil Sci. Soc. Am. J.* **2000**, *64*, 1443–1454. [CrossRef]
2. Mazur, A. Quantity and Quality of Surface and Subsurface Runoff from an Eroded Loess Slope Used for Agricultural Purposes. *Water* **2018**, *10*, 1132. [CrossRef]
3. Hladký, J.; Novotná, J.; Elbl, J.; Kynický, J.; Juřička, D.; Novotná, J.; Brtnický, M. Impacts of Water Erosion on Soil Physical Properties. *Acta Univ. Agric. Silvic. Mendel. Brun.* **2016**, *64*, 1523–1527. [CrossRef]
4. Duan, X.; Xie, Y.; Ou, T.; Lu, H. Effects of soil erosion on long-term soil productivity in the black soil region of northeastern China. *Catena* **2011**, *87*, 268–275. [CrossRef]
5. Arriaga, F.J.; Lowery, B. Corn production on an eroded soil: Effects of total rainfall and soil water storage. *Soil Tillage Res.* **2003**, *71*, 87–93. [CrossRef]
6. Asiedu, J.K. Assessing the Threat of Erosion to Nature-Based Interventions for Stormwater Management and Flood Control in the Greater Accra Metropolitan Area, Ghana. *J. Ecol. Eng.* **2018**, *19*, 1–13. [CrossRef]
7. Mioduszewski, W. *Low Retention. Protection of Water Resources and Natural Environment*; IMUZ: Falenty, Poland, 2003. (In Polish)
8. Alaoui, A.; Rogger, M.; Peth, S.; Bloschl, G. Does soil compaction increase floods? A review. *J. Hydrol.* **2018**, *557*, 631–642. [CrossRef]
9. Bluett, C.; Tullberg, J.N.; McPhee, J.E.; Antille, D.L. Soil and tillage research: Why still focus on soil compaction? *Soil Till. Res.* **2019**, *194*. [CrossRef]
10. Smoroń, S. The Risk of Surface Waters Eutrophication in Loessial Uplands of Małopolska. *Woda Środ. Obsz. Wiej.* **2012**, *12*, 181–191. Available online: http://yadda.icm.edu.pl/yadda/element/bwmeta1.element.baztech-article-BATC-0008-0029 (accessed on 20 April 2021).
11. Olson, K.R.; Gennadiyew, A.N.; Jones, R.L.; Chernyanskii, S. Erosion pattern on cultivated and reforested hillslopes in Moscow Region, Russia. *Soil Sci. Soc. Am. J.* **2002**, *66*, 193–201. [CrossRef]
12. Pimentel, D.; Allen, J.; Beers, A.; Guinand, L.; Hawkins, A.; Linder, R.; McLanghlin, P.; Meer, B.; Musonda, D.; Perdue, D.; et al. Soil erosion and agricultural productivity. In *World Soil Erosion and Conservation*; David, P., Ed.; Cambridge University Press: Cambridge, UK, 1993.
13. Seybold, C.A.; Herrick, J.E.; Brejda, J.J. Soil resilience: A fundamental component of soil quality. *Soil Sci.* **1999**, *164*, 224–234. [CrossRef]

14. Catt, J.A. The agricultural importance of loess. *Earth-Sci. Rev.* **2001**, *54*, 213–229. [CrossRef]
15. Józefaciuk, C.; Józefaciuk, A.; Nowocień, E.; Wawer, R. Structure of soil hazard with surface water erosion in the Zachodniopomorskie Voivodeship. *Folia Univ. Agric. Stetin. Agric.* **2001**, *87*, 285–290. Available online: http://yadda.icm.edu.pl/yadda/element/bwmeta1.element.agro-article-38990215-ab59-49ee-a459-eb2f377229d6?q=bwmeta1.element.agro-volume-3b5c3bd3-025b-4231-baad-1d6667682f21;10&qt=CHILDREN-STATELESS (accessed on 21 April 2021). (In Polish)
16. Zajączkowski, K.; Tałałaj, Z.; Węgorek, T.; Zajączkowska, B. *Selection of Trees and Shrubs for Planting in Rural Areas*; IBL: Warsaw, Poland, 2001. (In Polish)
17. Achim, E.; Manea, G.; Vijulie, I.; Cocos, O.; Tîrla, L. Ecological reconstruction of the plain areas prone to climate aridity through forest protection belts. Case study: Dabuleni Town, Oltenia Plain, Romania. *Procedia Environ. Sci.* **2012**, *14*, 154–163. [CrossRef]
18. Mazur, Z.; Pałys, S.; Węgorek, T. The anti-erosion function of ribbon fields and strip canopies on rangelands. *Zesz. Probl. Post. Nauk Roln.* **1985**, *311*, 159–168. (In Polish)
19. Liu, W.; Mi, J.; Song, Z.; Yan, J.; Li, J.; Sang, T. Long-term water balance and sustainable production of Miscanthus energy crops in the Loess Plateau of China. *Biomass Bioenergy* **2014**, *62*, 47–57. [CrossRef]
20. Xue, S.; Lewandowski, I.; Kalinina, O. Miscanthus establishment and management on permanent grassland in southwest Germany. *Ind. Crop. Prod.* **2017**, *108*, 572–582. [CrossRef]
21. Ben Fradj, N.; Rozakis, S.; Borzęcka, M.; Matyka, M. Miscanthus in the European bio-economy: A network analysis. *Ind. Crop. Prod.* **2020**, *148*, 112281. [CrossRef]
22. Rusinowski, S.; Krzyżak, J.; Clifton-Brown, J.; Jensen, E.; Mos, M.; Webster, R.; Sitko, K.; Pogrzeba, M. New Miscanthus hybrids cultivated at a Polish metal-contaminated site demonstrate high stomatal regulation and reduced shoot Pb and Cd concentrations. *Environ. Pollut.* **2019**, *252*, 1377–1387. [CrossRef]
23. Winkler, B.; Mangold, A.; von Cossel, M.; Clifton-Brown, J.; Pogrzeba, M.; Lewandowski, I.; Iqbal, Y.; Kiesel, A. Implementing miscanthus into farming systems: A review of agronomic practices, capital and labour demand. *Renew. Sustain. Energy Rev.* **2020**, *132*, 110053. [CrossRef]
24. Clifton-Brown, J.; Schwarz, K.U.; Awty-Carroll, D.; Iurato, A.; Meyer, H.; Greef, J.; Gwyn, J.; Mos, M.; Ashman, C.; Hayes, C.; et al. Breeding Strategies to Improve Miscanthus as a Sustainable Source of Biomass for Bioenergy and Biorenewable Products. *Agronomy* **2019**, *9*, 673. [CrossRef]
25. Kowalczyk-Juśko, A. Chemical composition and energetic characteristics of *Miscanthus sacchariflorus* biomass as used for generation of energy. *Przem. Chem.* **2016**, *95/11*, 2326–2329. [CrossRef]
26. Klimiuk, E.; Pokój, T.; Budzyński, W.; Dubis, B. Theoretical and observed biogas production from plant biomass of different fibre contents. *Bioresour Technol.* **2010**, *101*, 9527–9535. [CrossRef]
27. Kowalczyk-Juśko, A.; Pochwatka, P.; Zaborowicz, M.; Czekała, W.; Mazurkiewicz, J.; Mazur, A.; Janczak, D.; Marczuk, A.; Dach, J. Energy value estimation of silages for substrate in biogas plants using an artificial neural network. *Energy* **2020**, *202*, 117729. [CrossRef]
28. Xie, L.; MacDonald, S.L.; Auffhammer, M.; Jaiswal, D.; Berck, P. Environment or food: Modeling future land use patterns of miscanthus for bioenergy using fine scale data. *Ecol. Econ.* **2019**, *161*, 225.e36. [CrossRef]
29. Kondracki, J. *Regional Geography of Poland*; PWN Warsaw: Warsaw, Poland, 2000. (In Polish)
30. Polish Society of Soil Science. Systematics of Polish soils. *Roczn. Gleb.* **2011**, *62*. Available online: http://ssa.ptg.sggw.pl/files/artykuly/2011_62/2011_tom_62_3/tom_62_3_calosc.pdf (accessed on 11 April 2021). (In Polish)
31. Ostrowska, A.; Gawliński, S.; Szczubiałka, Z. *Methods of Analysis and Assessment of Soil and Plant Properties-Catalog*; Inst. Ochr. Środ: Warsaw, Poland, 1991. (In Polish)
32. Van Reeuwijk, L.P. *Procedures for Soil Analysis*; ISRIC, World Soil Information: Wageningen, The Netherlands, 2002.
33. EN ISO 18134-3:2015. *Solid Biofuels—Determination of Moisture Content—Oven Dry Method—Part 3: Moisture in General Analysis Sample*. Available online: https://www.iso.org/standard/61637.html (accessed on 20 April 2021).
34. Brański, J. Determination of the amount of suspension by gravimetric method, direct using filters. *Pr. Inst. Hydrol. Melior.* **1969**, *94*, 13–21. (In Polish)
35. Hermanowicz, W.; Dojlido, W.; Dożańska, W.; Kosiorowski, B.; Zerbe, J. *Physico-Chemical Testing of Water and Sewage*; Arkady: Warsaw, Poland, 1999. (In Polish)
36. Mazur, Z.; Pałys, S. *Water Erosion of Soils in the Loess of Western Roztocze in 1988–1990 on the Example of a Fragment of the Por River Basin*; AR in Lublin: Lublin, Poland, 1991. (In Polish)
37. Rejman, J. Effect of Water and Tillage Erosion on Transformation of Soils and Loess Slopes. *Acta Agrophys.* **2006**, *136*. Available online: http://www.old.acta-agrophysica.org/artykuly/acta_agrophysica/ActaAgr_136_2006_0_0_0.pdf (accessed on 20 March 2021).
38. Price, K.; Jackson, C.R.; Parker, A.J. Variation of surficial soil hydraulic properties across land uses in the southern Blue Ridge Mountains, North Carolina, USA. *J. Hydrol.* **2010**, *383*, 256–268. [CrossRef]
39. Wang, Y.Q.; Shao, M.A. Spatial variability of soil physical properties in a region of the loess plateau of PR China subject to wind and water erosion. *Land Degrad. Develop.* **2011**, *24*, 296–304. [CrossRef]
40. Turski, R.; Słowińska-Jurkiewicz, A.; Paluszek, J. The effect of erosion on the spatial differentation of the physical prperties of Orthic Luvisols. *Int. Agrophys.* **1992**, *6*, 123–136. Available online: http://www.international-agrophysics.org/The-effect-of-erosion-on-the-spatial-differentiation-of-the-physical-properties-of,127853,0,2.html (accessed on 27 April 2021).

41. Edwards, L.M.; Burney, J.R. The effect of antecedent freeze-thaw frequency on runoff and soil loss from frozen soil with and without subsoil compaction and ground cover. *Can. J. Soil Sci.* **1989**, *69*, 799–811. Available online: https://cdnsciencepub.com/doi/pdf/10.4141/cjss89-080 (accessed on 17 April 2021). [CrossRef]
42. Wang, Y.; Zhang, B. Chapter Four—Interception of Subsurface Lateral Flow Through Enhanced Vertical Preferential Flow in an Agroforestry System Observed Using Dye-Tracing and Rainfall Simulation Experiments. *Adv. Agron.* **2017**, *142*, 99–118. [CrossRef]
43. Monti, A.; Zatta, A. Root distribution and soil moisture retrieval in perennial and annual energy crops in Northern Italy. *Agric. Ecosyst. Environ.* **2009**, *132*, 252–25930. [CrossRef]
44. Mann, J.J.; Barney, J.N.; Kyser, G.B.; DiTomaso, J.M. Root system dynamics of *Miscanthus* x *giganteus* and *Panicum virgatum* in response to rainfed and irrigated conditions in California. *Bioenerg. Res.* **2013**, *6*, 678–687. [CrossRef]
45. Neukirchen, D.; Himken, M.; Lammel, J.; Czyionka-Krause, U.; Olfs, H.W. Spatial and temporal distribution of the root system and root nutrient content of an established *Miscanthus* crop. *Eur. J. Agron.* **1999**, *11*, 301–309. [CrossRef]
46. Ma, B.; Yu, X.; Ma, F.; Li, Z.; Wu, F. Effects of crop canopies on rain splash detachment. *PLoS ONE* **2014**, *9*, e99717. [CrossRef]
47. Bochet, E.; Poesen, J.; Rubio, J.L. Influence of plant morphology on splash erosion in a Mediterranean matorral. *Z. Geomorphol.* **2002**, *46*, 223–243. [CrossRef]
48. Święchowicz, J. *Rainfall Thresholds for Erosion Processes in Agricultural Catchments*; Instytut Geografii i Gospodarki Przestrzennej Uniwersytetu Jagiellońskiego: Kraków, Poland, 2012. Available online: http://www.pinap.geo.uj.edu.pl/publikacje.php?pdf=000130-097& (accessed on 20 April 2021). (In Polish)
49. Żmuda, R. Fluvial Transport System Functioning in Small Catchment Threatened by Soil Water Erosion. *Zesz. Nauk. Akad. Rol. Wrocławiu* **2006**, *544*. Available online: https://www.dbc.wroc.pl/dlibra/doccontent?id=3284 (accessed on 17 April 2021). (In Polish)
50. Mucha, J. *Geostatistical Methods in the Documentation of Deposits*; AGH w Krakowie: Kraków, Poland, 1994. (In Polish)
51. Kim, K.; Kim, B.; Eum, J.; Seo, B.; Christopher, L.; Shope, C.L.; Peiffer, S. Impacts of land use change and summer monsoon on nutrients and sediment exports from an agricultural catchment. *Water* **2018**, *10*, 544. [CrossRef]
52. Zhang, F.; Wang, J.; Wang, X. Recognizing the relationship between spatial patterns in water quality and land-use/cover types: A case study of the Jinghe Oasis in Xinjiang, China. *Water* **2018**, *10*, 646. [CrossRef]
53. Sharpley, A.N. The selective erosion of plant nutrients in runoff. *Soil Sci. Soc. Am. J.* **1985**, *49*, 1527–1534. [CrossRef]
54. Berger, C.; Schulze, M.; Rieke-Zapp, D.; Schlunegger, F. Rill development and soil erosion: A laboratory study of slope and rainfall intensity. *Earth Surf. Process. Landf.* **2010**, *35*, 1456–1467. [CrossRef]
55. Wang, Y.-C.; Lai, C.-C. Evaluating the erosion process from a single-stripe laser-scanned topography: A laboratory case study. *Water* **2018**, *10*, 956. [CrossRef]
56. Gil, E. The role of land use in the course of surface runoff and rinsing on flysch slopes. *Przegląd Geograficzny* **1986**, *58*, 51–65. Available online: http://rcin.org.pl/Content/13228/WA51_16244_r1986-t58-z1-2_Przeg-Geogr.pdf (accessed on 15 April 2021). (In Polish)
57. Gil, E. Water circulation and rinsing on flysch slopes used for agricultural purposes in the years 1980–1990. *Zesz. IGiPZ PAN* **1999**, *60*, 1–77. Available online: https://rcin.org.pl/igipz/Content/34427/WA51_44671_r1999-nr60_Zeszyty-IGiPZ.pdf (accessed on 14 April 2021). (In Polish)
58. Regulation of the Minister of Maritime Affairs and Inland Navigation of October 11, 2019 on the Classification of Ecological Status, Ecological Potential and Chemical Status and the Method of Classifying the Status of Surface Water Bodies, as well as Environmental Quality Standards for Priority Substances. Available online: https://isap.sejm.gov.pl/isap.nsf/download.xsp/WDU20190002149/O/D20192149.pdf (accessed on 22 April 2021). (In Polish)
59. Dupas, R.; Delmas, M.; Dorioz, J.M.; Garnier, J.; Moatar, F.; Gascuel-Odoux, C. Assessing the impact of agricultural pressures on N and P loads and eutrophication risk. *Ecol. Indic.* **2015**, *48*, 396–407. [CrossRef]
60. Shainberg, I.; Mamedow, A.I.; Levy, G.J. Role of Wetting Rate and Rain Energy in Seal Formation and Erosion. *Soil Sci.* **2003**, *168*, 54–62. Available online: https://journals.lww.com/soilsci/Abstract/2003/01000/ROLE_OF_WETTING_RATE_AND_RAIN_ENERGY_IN_SEAL.7.as (accessed on 14 April 2021). [CrossRef]
61. Koc, J. The effect of the intensity of the area's use on the amount of nutrients outflow from agricultural areas. *Roczn. AR w Poznaniu* **1998**, *52*, 101–106. (In Polish)
62. Rajda, W.; Ostrowski, K.; Kowalik, T.; Marzec, J. Chemical erosion in agricultural micro-watersheds in the areas at the mountain feet. *Rocz. AR w Poznaniu* **1994**, *266*, 139–152. (In Polish)
63. Stanisz, A. *Accessible Statistics Course*; StatSoft Polska Sp. z o.o.: Kraków, Poland, 1998. (In Polish)
64. Azuka, C.V.; Igué, A.M. Surface runoff as influenced by slope position and land use in the Koupendri catchment of northwest Benin: Field observation and model validation. *Hydrol. Sci. J.* **2020**, *65*, 995–1004. [CrossRef]
65. Jourgholami, M.; Karami, S.; Tavankar, F.; Lo Monaco, A.; Picchio, R. Effects of Slope Gradient on Runoff and Sediment Yield on Machine-Induced Compacted Soil inTemperate Forests. *Forests* **2021**, *12*, 49. [CrossRef]
66. Field, J.P.; Breshears, D.D.; Whicker, J.J. Toward a more holistic perspective of soil erosion: Why aeolian research needs to explicitly consider fluvial processes and interactions. *Aeolian Res.* **2009**, *1*, 9–17. [CrossRef]
67. Mazur, A. Water erosion in the agricultural loess catchment with a periodical water outflow in Wielkopole (Lubelskie Upland) in the years 2008–2011. *Inżynieria Ecol.* **2018**, *19*, 121–132. [CrossRef]